Science of the Total Environment xxx (xxxx) 154424

Contents lists available at ScienceDirect

Science of the Total Environment

journal homepage: www.elsevier.com

Application of hydrochemical and multi-isotopic ($^{87}Sr/^{86}Sr$, $\delta^{13}C$-DIC, $\delta^{2}H$-H_2O, $\delta^{18}O$-H_2O) tools to determine contamination sources and processes in the Guadalhorce River Basin, southern Spain

M. Glok-Galli [a, b], I. Vadillo-Pérez [c, *], P. Jiménez-Gavilán [c], L. Ojeda [c], B. Urresti-Estala [d], D.E. Martínez [b, e]

[a] Faculty of Engineering, National University of the Center of Buenos Aires Province, 7400 Olavarría, Argentina
[b] National Scientific and Technical Research Council, Argentina
[c] Group of Hydrogeology, Department of Geology, Faculty of Science, University of Malaga, 29071 Malaga, Spain
[d] TRAGSA, c/Parsi 5, 8, 41016 Seville, Spain
[e] Group of Hydrogeology, University of Mar del Plata, 7600 Mar del Plata, Argentina

ARTICLE INFO

Editor: Jurgen Mahlknecht

Keywords:
Hydrochemistry
Strontium isotopes
Water isotopes
Carbon isotope
Water pollution
Guadalhorce River Basin

ABSTRACT

The integrated use of multi-isotopic ($^{87}Sr/^{86}Sr$, $\delta^{13}C$-DIC, $\delta^{2}H$-H_2O, $\delta^{18}O$-H_2O) and hydrochemical data was applied in the highly anthropized Guadalhorce river basin, southern Spain, to improve the knowledge about water contamination sources and processes and to achieve improved water resource management. The results obtained highlight the importance of the use of isotopes as tracers of pollutants. DIC, $\delta^{2}H$-H_2O, $\delta^{18}O$-H_2O and $\delta^{13}C$-DIC allowed differentiating two water recharge end members: direct rainwater, infiltrated into the upper and lower detritic aquifers of the sub-basins, and the Guadalhorce dam system, which act as a source in some groundwater and surface waters of the lower sub-basin. $^{87}Sr/^{86}Sr$ data supported the existing conclusions in relation to pollution sources in the study area. The Triassic basement (evaporites) of the carbonate and detritic aquifers of the basin generally controls the natural $^{87}Sr/^{86}Sr$ composition in waters of the upper sub-basin. Only one groundwater sample reflects the influence of a human organic source (sewage) in its composition. On the other hand, mixing of human inorganic (fertilizers and detergents) strontium sources is required to explain the $^{87}Sr/^{86}Sr$ contents of the lower sub-basin waters. Discriminating the use of domestic detergents as another anthropogenic source of strontium and sulphate in waters is a novel finding in this research. The conclusions reached can be extrapolated to other anthropized basins.

1. Introduction

Groundwater is a strategic but scarce resource in the Mediterranean Basin because of the arid and semi-arid climatic conditions and the drought periods occurring periodically in this region (Durán Valsero, 2007). In this framework, climate change and related extreme events indeed exacerbate the negative trend in water quality (Barbieri et al., 2021). This area is an agricultural zone *par excellence*, in addition to one that is experiencing growth in tourism and urban development, which increases the water demand needed to satisfy these new uses. Groundwater is as well an important geological agent and constitutes one of the fundamental pillars for the maintenance and existence of natural landscapes and terrestrial aquatic ecosystems. It is a fundamental element in the hydrological cycle and plays a key role as the base flow of wetlands and rivers (Winter, 1999). As a result of this close relationship, deterioration of groundwater quality directly affects surface water and dependent terrestrial ecosystems, making its preservation of utmost importance from an environmental standpoint.

In the Guadalhorce River Basin (GRB) (Fig. 1), a basin in southern Spain representative of the Western Mediterranean, aquifer water is the main supply for different uses. In this area, the presence of different lithogenic sources (carbonate detrital and evaporitic materials) and the existence of potential diffuse and point anthropogenic sources (Fig. 2) are both responsible for the ultimate chemical quality of water bodies. Human pressure results from the existence of multiple economic activities in the area, facilitated by the geographic, geomorphologic, climatic

* Corresponding author.
E-mail addresses: glokgalli@mdp.edu.ar (M. Glok-Galli), Vadillo@uma.es (I. Vadillo-Pérez), pgavilan@uma.es (P. Jiménez-Gavilán), luciaor@uma.es (L. Ojeda), murresti@tragsa.es (B. Urresti-Estala), demarti@mdp.edu.ar (D.E. Martínez).

https://doi.org/10.1016/j.scitotenv.2022.154424
Received 22 December 2021; Received in revised form 20 February 2022; Accepted 5 March 2022
0048-9697/

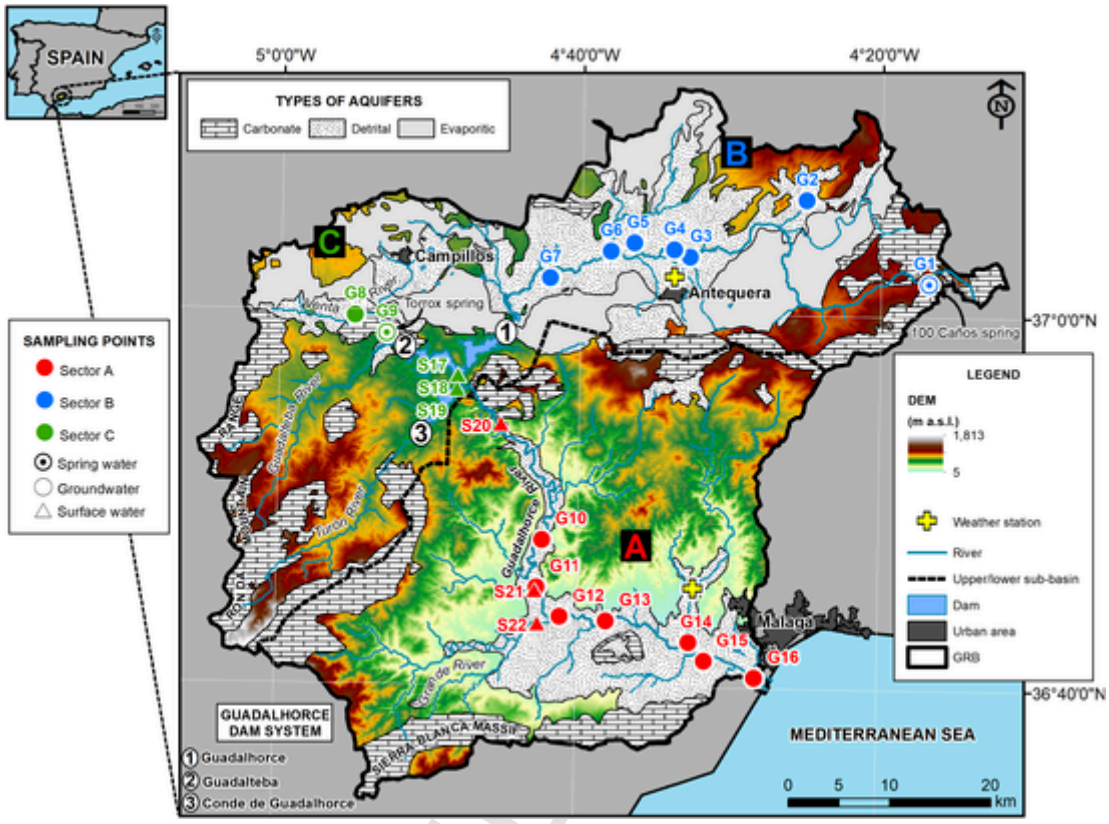

Fig. 1. Location map of the Guadalhorce River Basin (GRB) (DEM:: Digital Elevation Model in meters above sea level -m a.s.l.-).

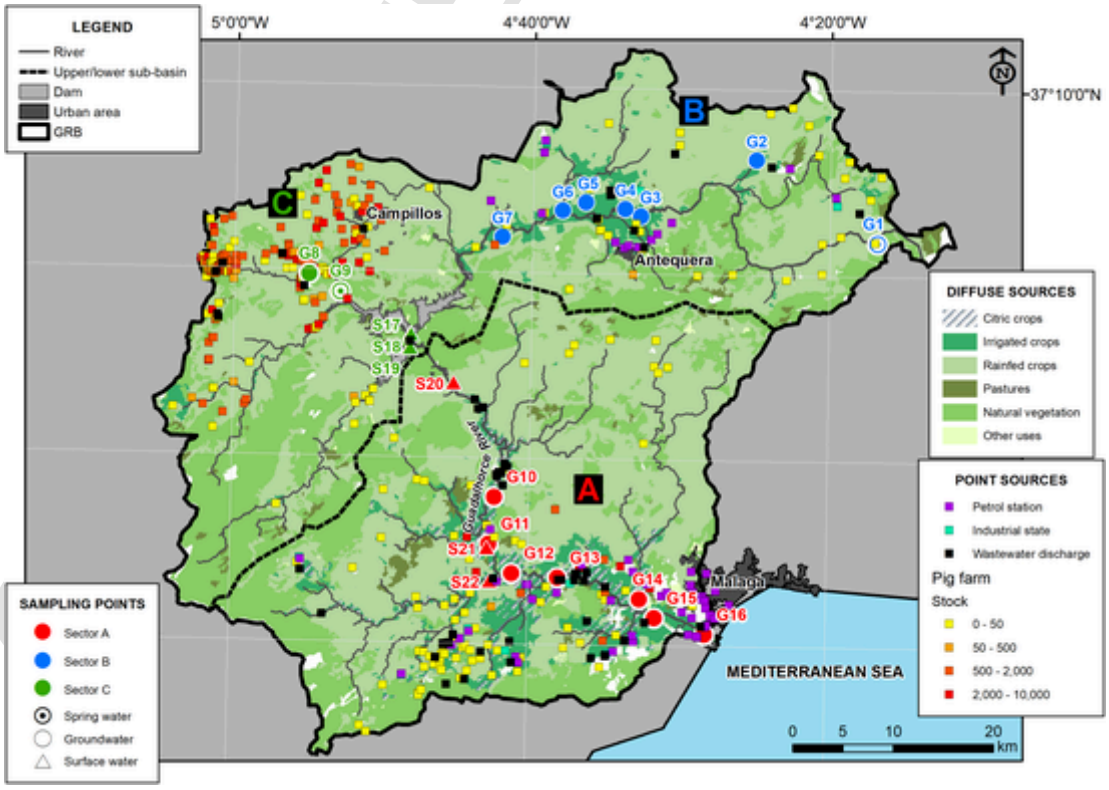

Fig. 2. Main diffuse and point pollution sources in the Guadalhorce River Basin (GRB) (data from Sánchez-García, 2010, 2013; BOJA, 2013).

and socio-cultural context coupled with its proximity to major population centers, including the city of Malaga. As the main source of water demand in the GRB, agricultural activities use 75% of the total volume of this resource (approximately 255 million m^3 per year), while urban water supply accounts for the remaining demand (85 million m^3 per year) (BOJA, 2013). The widespread use of chemical fertilizers (containing NH_4NO_3, $NH_4NO_3SO_4$, KNO_3, H_3PO_4 and $(NH_4)_2SO_4$, among other salts) and pig manure are the main impacts identified, which are responsible for the nitrate and sulphate input. Other impacts are evidenced by the presence of pesticides, salinization (by marine intrusion or groundwater over-exploitation) and pollution from urban or industrial origins (wastewater) (Sánchez-García et al., 2007; Carrasco-Cantos et al., 2008; MAGRAMA, 2012; Sánchez-García, 2010, 2013; Urresti-Estala et al., 2015, 2016).

The identification of possible contamination sources (natural and/or anthropic) and the interpretation of hydrological and biogeochemical processes linked to pollution scenarios can be achieved through the use of isotopic techniques (Clark and Fritz, 1997; Mook, 2002). The potential impact of some existing pollutants in water can be recognized due to the presence of isotopes either directly ($\delta^{34}S$-SO_4, $\delta^{18}O$-SO_4, $\delta^{15}N$-NO_3, $\delta^{18}O$-NO_3, $\delta^{13}C$-DIC, $^{87}Sr/^{86}Sr$), indirectly (δ^2H-H_2O, $\delta^{18}O$-H_2O) or in combination with chemical parameters (Cl^-, NO_3^-, SO_4^{2-}). In particular, water stable isotopes (δ^2H-H_2O and $\delta^{18}O$-H_2O) are employed as tracers to understand water dynamics, including groundwater-surface water interactions, recharge and discharge estimations, water mixing, flow lines and water residence times in aquifers (Clark and Fritz, 1997; Kendall and McDonnell, 1998; Cook and Herczeg, 1999; Geyh, 2000; Mook, 2002; Vitvar et al., 2005; Awaleh et al., 2022). Carbon-13 of dissolved inorganic carbon ($\delta^{13}C$-DIC) is another environmental stable isotope with diverse applications in hydrological studies. DIC and carbon dioxide gas ($CO_{2(g)}$) sources contributing to waters can be assessed using $\delta^{13}C$-DIC and $\delta^{13}C$-$CO_{2(g)}$ (Aravena and Robertson, 1998; Vitòria et al., 2008; Otero et al., 2009). In addition, strontium (Sr^{2+}) is a divalent cation that can replace calcium (Ca^{2+}) in the structure of minerals. The $^{87}Sr/^{86}Sr$ ratio is as well a very useful indicator in hydrological systems, the analysis and interpretation of which can help to understand and quantify mixing between different sources, whether natural or anthropogenic (Négrel et al., 2001; Soler et al., 2002; Petelet-Giraud et al., 2003; Tichomirowa et al., 2010; Clark, 2015; Glok-Galli et al., 2020).

The main goal of this study was to improve the knowledge of contamination sources and processes in groundwater and surface water of the highly anthropized GRB, through the application of a multi-isotopic approach ($^{87}Sr/^{86}Sr$, $\delta^{13}C$-DIC, δ^2H-H_2O, $\delta^{18}O$-H_2O) coupled with hydrochemical data. This will allow to evaluate the use of these isotopes as pollutant tracers and to improve water resource management, which is of paramount importance in this Mediterranean basin.

Several contributions exist as background information regarding the GRB that relate to many of the aspects considered. The integrated use of $\delta^{34}S$-SO_4 and $\delta^{18}O$-SO_4 isotopes was considered by Vadillo-Pérez et al. (2006) to characterize possible sulphate sources (natural or anthropogenic) and their contribution in different sectors of the catchment area. Sánchez-García et al. (2007) have studied contamination from agricultural activities present in the GRB and have considered the analysis of chemical data for the evaluation of nitrogen compound contents in groundwater together with their spatial distribution. Carrasco-Cantos et al. (2008) and Urresti-Estala et al. (2013) have interpreted the available hydrochemical information for the application of the European water framework directive within the GRB and for the determination of background levels of groundwater quality of groundwater bodies in this basin, respectively. In addition, the joint application of chemical data analysis and the use of environmental isotopes was reflected in the works of Urresti-Estala et al. (2015) and Urresti-Estala et al. (2016). In the former case, the use of $\delta^{34}S$-SO_4, $\delta^{18}O$-SO_4, $\delta^{15}N$-NO_3 and $\delta^{18}O$-NO_3 isotopes was highlighted and the natural background and contamination sources in the basin were determined. In the latter case, the authors have evaluated hydrochemical trends in the GRB, in terms of compliance with the European groundwater directive for 2015, considering the analysis of δ^2H-H_2O and $\delta^{18}O$-H_2O content. More recently, Llamas-Dios et al. (2020, 2021) have evaluated the occurrence and distribution of a wide range of Contaminants of Emerging Concern (CECs) and regulated organic pollutants in the studied basin, with the support of hydrochemical and isotopic (δ^2H-H_2O and $\delta^{18}O$-H_2O) tools. In these previous studies, the interpretation of $\delta^{13}C$-DIC and $^{87}Sr/^{86}Sr$ analyses in waters of the GRB has not been performed. As a result, this work becomes a novel approach in this research, one of potential interest to local resource managers.

2. Study area

The GRB located in southern Spain has an area of 3200 km^2, representing over 40% of the total surface of the province of Malaga (7308 km^2). The Guadalhorce River is the most important fluvial course of the province with a total length of 166 km and an average flow of 8 m^3/s. It begins in the northeast of the basin and flows into the Mediterranean Sea, to the southwest of the city of Malaga (Fig. 1). The climate in the area is characterized by mild temperatures, with an annual mean value varying from 13 to 18 °C. The wet season, with frequent extreme rainfall events, lasts from October to February and the driest season lasts from June to September. Rainfall values range from less than 400 mm/year in the southern sector of the basin to 1100 mm/year in the northern part (mountainous areas) (Carrasco-Cantos et al., 2008; Urresti-Estala et al., 2015, 2016; Llamas-Dios et al., 2020, 2021).

From a practical point of view, the GRB is divided into two sections due to the presence of a mountain range located in the center: the northern (upper) sub-basin, whose flatlands are located at a higher altitude (300–600 m a.s.l.), and the southern (lower) one (0–200 m a.s.l., as the altitude of its flatlands; Sánchez-García, 2010) (DEM in Fig. 1). The hydrological dynamic of the lower sub-basin is influenced by three dams collecting water from the entire upper basin: Guadalhorce, Guadalteba and Conde de Guadalhorce, which conform the Guadalhorce dam system (Fig. 1). These reservoirs are located at the confluence of the Guadalhorce River with its two larger tributaries (Turón and Guadalteba rivers) and sit in the NE foothills of the Ronda Mountain Range. The Conde de Guadalhorce dam is located in the Turón River, which drains the karstic area of the Ronda Mountain Range. The Guadalhorce dam, situated in the river bearing the same name, has its catchment area in the endorheic zone of Antequera and receives an average flow of 20 L/s of dense saline water (80–140 g/L) in its deep part from the Meliones spring, which is occasionally submerged. Lastly, the Guadalteba dam sits in an intermediate position, its drainage basin also lying in the endorheic area of Antequera and receiving some deepwater coming from the Guadalhorce reservoir (Armengol et al., 1990).

Groundwater bodies are associated with three types of aquifers: calcareous, detrital and evaporitic (Fig. 1). Carbonate aquifer springs feed the main surface watercourses. These are formed by Mesozoic limestones, dolostones and marbles of the External and Internal Zones of the Betic Cordillera. The Malaguide Complex, a tectonic unit included in the Internal Zone, lies on the right bank of the Guadalhorce River, near the city of Malaga, and contains greywackes and phyllites (shales) with disseminated pyrite and organic matter (Galvez and Orozco, 1979; Herbig, 1985).

As regards detrital aquifers, there are three water systems (referred to as groundwater bodies by the basin authority) situated in the flatlands of the basin: the Lower Guadalhorce (sector A), located in the lower part of the basin; Vega de Antequera-Archidona (sector B) and the Teba-Almargen-Campillos area (sector C), both of them located in the upper sub-basin (Fig. 1). In sector A, the Quaternary and unconfined aquifer consists of alluvial sediments such as gravels, sands, silts and clays. The underlying rocks are Upper Miocene calcareous sand-

stones and conglomerates, and Pliocene conglomerates, marl and sand layers. Pliocene sediment thicknesses can reach 300 m and conglomerates form a discontinuous confined aquifer at the bottom of the series, which underlay the marls. At a shallower level, interrupted sand layers form a semiconfined aquifer (Linares et al., 1995). In sector B, Neogene and Quaternary deposits such as calcareous sandstones and alluvial sediments constitute the unconfined aquifer (Carrasco-Cantos, 1986). Finally, sector C consists of two detritic aquifers and one carbonate aquifer that are hydrologically connected. The detritic aquifers consist of calcarenites, conglomerates and marls (Miocene) and detrital materials of fluvial origin (Quaternary), while the carbonate aquifer is formed by Jurassic limestones (Carrasco-Cantos et al., 2007).

The only evaporitic aquifer is in the northern sub-basin and comprises Triassic outcrops of clays, sandstones and evaporative materials (gypsum and halite). These materials also constitute the basement of the carbonate and detritic aquifers of the basin (Sánchez-García, 2010).

River-aquifer interactions take place throughout the basin, with some areas behaving as gaining rivers and others as losing ones. The Guadalhorce River in sector B is hydraulically connected with the porous aquifer, whereas the Venta River, in sector C, recharges the aquifers which ultimately drain through the Torrox spring outflowing into the dam. Surface water is eventually released downstream toward sector A through irrigation channels and to the Guadalhorce riverbed, where this river displays both a gaining and losing behavior (Durán Valsero, 2007; Urresti-Estala et al., 2015; Llamas-Dios et al., 2020).

Pressure on groundwater bodies of the GRB (Fig. 2) was considered similar as for surface water, in addition to abstraction and marine intrusion. The main pressures affecting groundwater bodies in carbonate aquifers derive from the pumping of water to supply nearby towns and villages. This process leads to important falls in piezometric levels. Other localized pressures are caused by urban solid waste landfills, petrol stations and campsites. Groundwater bodies located in evaporite aquifers are subjected to very few pressures except agricultural activity, which usually occurs without any irrigation and is less developed here, as well as local sources of pollution, such as petrol stations and light industry. Water bodies located in detrital aquifers are subjected to pressures caused by agricultural activity and by significant livestock farming in the northwestern sector, which generates pollution by nitrates and organic components, as mentioned. The numerous pumping abstraction points in these areas for irrigation purposes also generate falls in piezometric levels. In coastal areas, pumping may enable marine intrusion (Carrasco-Cantos et al., 2008).

3. Materials and methods

A summary of the proposed methodological framework and the innovative conclusions of this new study are displayed in Fig. 3.

A compilation of pre-existing data and information related to the study area (climatological, topographical, geological, hydrogeological, land use, hydrochemical, isotopical, CECs) was done. In order to update the hydrochemical and water isotopes data and improve the knowledge of contamination sources and processes in waters of the GRB, a sampling campaign was conducted in June 2017. This year, temperature mean values varied between 6.3 and 26.7 °C, and monthly accumulated rainfall values ranged from 0 to 78 mm (November) and 123.2 mm (February) in the northern and southern part of the basin, respectively (see location of weather stations in Fig. 1). The null precipitation value corresponded to the month in which samples were collected. These climatic conditions and the current ones are similar (https://www.juntadeandalucia.es/agriculturaypesca/ifapa/riaweb/web/).

Two samples from springs draining carbonate aquifers and outflowing into the main water courses were collected in the upper sub-basin (sample G1 from the 100 Caños spring in sector B -~825 m a.s.l.- and sample G9 from the Torrox spring in sector C -~365 m a.s.l.-). Most groundwater samples belonging to detrital aquifers were collected from fourteen private irrigation wells (< 40 m deep), directly after continuous pumping or using a submersible sampler: seven samples were collected in the upper sub-basin (samples G2–G7 in sector B and sample G8

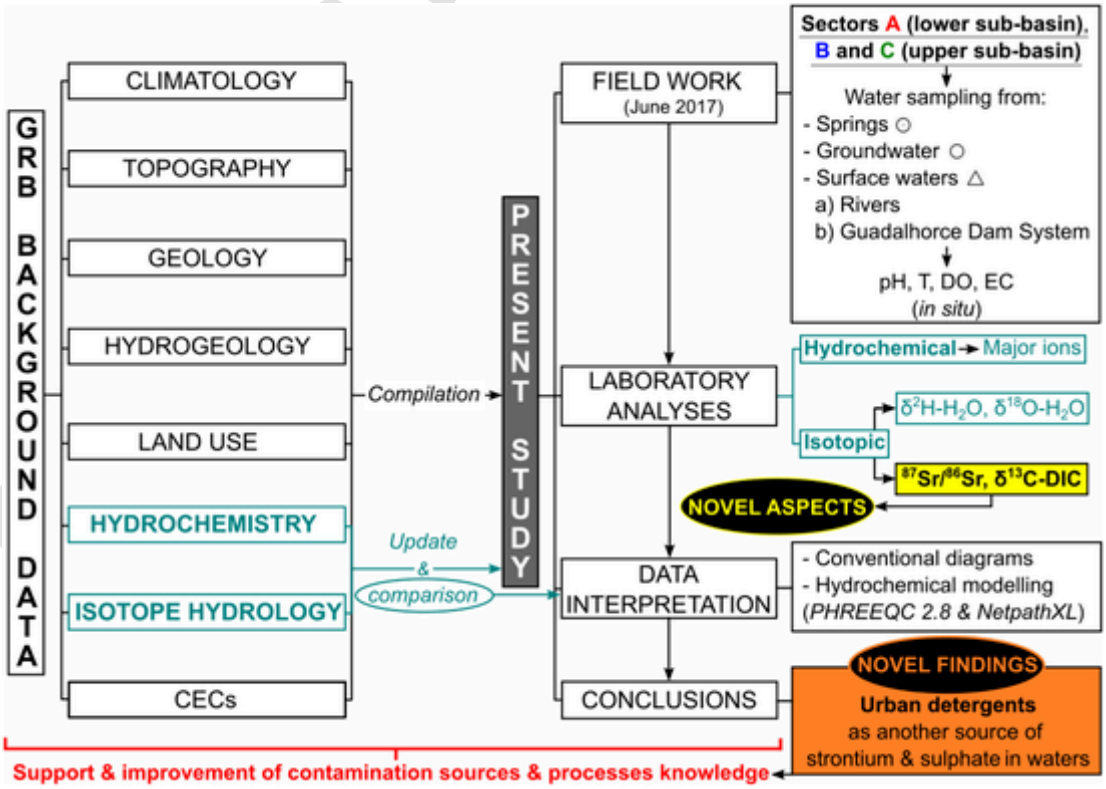

Fig. 3. Summary of the proposed methodological framework and the main conclusions of the present study (GRB: Guadalhorce River Basin; CECs: Contaminants of Emerging Concern; T: temperature; DO: dissolved oxygen; EC: electrical conductivity. See location of sampling points in Fig. 1).

in sector C) and seven in the lower one -sector A- (samples G10–G16). Moreover, six surface water samples were collected: three from the dams in sector C (samples S17, S18 and S19) and three from rivers/channel in sector A (samples S20, S21 and S22) (Fig. 1). All water samples were filtered through a 0.45 μm Millipore® (Merck KGaA, Darmstadt, Germany) filter. Samples for hydrochemical (Ca^{2+}, Mg^{2+}, Na^{+}, K^{+}, Cl^{-}, HCO_3^{-}, CO_3^{2-}, SO_4^{2-}, NO_3^{-} and Sr^{2+}) and isotopic (δ^2H-H_2O, $\delta^{18}O$-H_2O and $\delta^{13}C$-DIC) analyses were stored in sterile high-density polyethylene bottles (120 mL) sealed with inverted cone caps. Samples for $^{87}Sr/^{86}Sr$ analyses were collected in new 1 L polyethylene bottles with double cap. All bottles were rinsed before sampling, carried in a cool-box and stored in a fridge (<4 °C) until analysis, generally performed within 24 h after sampling. A portable multi-parameter probe (Hach-Lange HQ40d; Hach, Loveland, CO, USA) was used to measure in situ physico-chemical parameters: pH, temperature, dissolved oxygen (DO) and electrical conductivity (EC).

Chemical and isotopic (δ^2H-H_2O, $\delta^{18}O$-H_2O, $\delta^{13}C$-DIC) analyses were conducted at the laboratory of the Center for Hydrogeology of the University of Malaga, Spain. Major and minor water ions were determined using a 881 Compact IC Pro (HPLC), with a precision of ±0.1 mg/L. A variation coefficient of <5% was considered. DIC content was determined from the sum of HCO_3^{-} and CO_3^{2-}.

δ^2H-H_2O and $\delta^{18}O$-H_2O analyses were determined in a Picarro Water Isotope Analyzer L2120i (laser spectroscopy). The results were expressed as δ values permill (‰), defined as: $\delta = 1000\,(R_s - R_p)/R_p$ ‰; where δ is the isotopic deviation in ‰; S is the sample; P is the international reference; and R is the isotopic ratio ($^2H/^1H$ and $^{18}O/^{16}O$ in this case), in accordance with the Vienna Standard Mean Oceanic Water (V-SMOW) international standards (Gonfiantini, 1978). The accuracy of isotope measurements was ±0.1‰ for $\delta^{18}O$ and ±1‰ for δ^2H. The local meteoric water line (LMWL) obtained by Barberá Fornell et al. (2018) was considered in this work. This LMWL was obtained for a period extending from 1961 to 2009 by means of orthogonal regression analysis from 252 monthly precipitation composite samples from the Gibraltar rainfall station (36°09′00″ N, 5°21′00″ W; 5 m a.s.l.), taken as the closest reference (~136 km from Malaga city) for the lower sub-basin. This is included in the Global Network of Isotopes in Precipitation (GNIP) (IAEA, 2017).

The $\delta^{13}C$-DIC analyses were performed using a GasBench-II headspace autosampler in line with a Delta V Advantage mass spectrometer (Thermo Scientifics, Bremen, Germany). Laboratory standards were calibrated against NIST Standard Reference Materials (NBS-19, NBS-18 and LSVEC). The analytical error was ±0.1‰.

The $^{87}Sr/^{86}Sr$ isotopic ratios were analyzed at the Geochronology and Isotope Geochemistry Unit at the Research Support Center of the University of Madrid, Spain, using a TIMS-Phoenix mass spectrometer. The Sr isotope standard was NBS 987 ($^{87}Sr/^{86}Sr$ = 0.710248 ± 0.000003, NBS1982, National Bureau of Standards Certificate of Analysis Standard Reference Material 987). The analytical error was ±0.01%.

3.1. Codes and modelling

PHREEQC 2.8 software (Parkhurst and Appelo, 1999) was used for the calculation of the calcite and strontianite saturation indexes (SI_{cal} and SI_{str}, respectively). On the other hand, an inverse model was prepared for the sector of the lower sub-basin located near the coast using the NetpathXL code, Version 1.5 (Plummer et al., 1994; Parkhurst and Charlton, 2008), considering that this is a useful tool for analyzing seawater intrusion, which is one of the pressure vectors acting on groundwater bodies in the southern part of sector A (Carrasco-Cantos et al., 2008).

The reactant phases included in the model were: calcite, $CO_{2(g)}$, iron sulphide (Fe-S), K-montmorillonite, the ionic exchange of Ca^{2+}, Mg^{2+} and Na^{+}, and strontianite (mass transfers indicated in mmol/L). These were selected from the analysis of the chemical data: 1) a $CO_{2(atm)}$ open system can be assumed from the unconfined nature of the Quaternary aquifer; 2) the clay-size particle percentage in the sediments, which triggers a higher exchange capacity; 3) the presence of calcareous sediments in the geological units under study; 4) sulphate reduction, which is a typical reaction in some saltwater/freshwater mixing zones in marine intrusion areas; and 5) the previous investigations conducted in the area (Luque Espinar et al., 2003; Urresti-Estala et al., 2016; Llamas-Dios et al., 2020, 2021).

The mixture of seawater and a groundwater sample (G13; Fig. 1), taken as freshwater due to its lowest EC value (and low Cl^{-} content), was considered as the initial solution and the groundwater sampling point situated nearest to the coast (G16; Fig. 1), as the final one. The conservative Cl^{-} ion that was not included in any of the phases was used to calculate the fraction of seawater in sample G16 (f_{sw} = 4%) according to the formula (Appelo and Postma, 2005): $f_{sw} = C_{Cl,sam} - C_{Cl,f} / C_{Cl,sw} - C_{Cl,f}$, where $C_{Cl,sam}$, $C_{Cl,f}$ and $C_{Cl,sw}$ refer to the Cl^{-} content in the mixing water (sample G16), freshwater (sample G13) and seawater, respectively.

The isotopic data was inserted in the NetpathXL files database. These inputs were not used as constraints in the mass balance models because it is known that several phases (calcite, Fe-S, strontianite) can precipitate in a seawater/freshwater mixing context (Nadler et al., 1980; Bosch and Custodio, 1993; Martínez and Bocanegra, 2002), being both sources and sinks for isotopes along the water flow path. Therefore, it is usually not valid to include isotopes as constraints in the mass balance, regardless of the value of the fractionation factor (Plummer et al., 1994). The problem was then treated as a Rayleigh distillation problem and computed and observed isotopic values could be compared to examine differences between the fractionating differential problem of isotopic evolution and the mass-balance result. Seawater stable isotopes composition was taken from the works of Spooner (1976), Clark and Fritz (1997), Mook (2002), Seal (2006) and Cheng et al. (2019).

Finally, in the absence of measurements, the NetpathXL code was also employed for the calculation of $\delta^{13}C$-$CO_{2(g)}$ values of water samples, taking into account a completely open system (gas-solution equilibrium). Samples information and the results of hydrochemical (plus the SI_{cal} and SI_{str} calculation) and isotopic analyses (plus $\delta^{13}C$-$CO_{2(g)}$ values obtained by the NetpathXL code) are shown in Tables A.1 and A.2 of the Supplementary material, respectively.

4. Results

4.1. Hydrochemical characterization

For all analyzed samples, pH values ranged from 6.2 to slightly alkaline. The maximum value of 9.6 was recorded in sector A, sample G16 (located near the coastline), where the minimum value of DO (1.5 mg/L) was also measured. EC values obtained were up to 3610, 1772 and 3980 μS/cm in sectors A (sample G10), B (sample G7) and C (sample S17), respectively. For Sr^{2+}, mean contents in waters were 1.5 mg/L in sector A, 3.0 mg/L in sector B and 2.4 mg/L in sector C (Table A.1). The hydrochemical facies analysis conducted using a Piper diagram (Back, 1961) (Fig. 4) revealed the presence of mixed types of waters in all sectors under study. In particular in sector A, the chemical composition of G16, located near the mouth of the Guadalhorce River (as mentioned above), and S20, collected from an irrigation channel located in its upper part, is of Cl^{-}-Na^{+} type. Conversely, sample S22, collected from the Grande River, is of HCO_3^{-}-Mg^{2+} type. This sampling point showed the lowest Sr^{2+} content (0.5 mg/L; Table A.1). Groundwater in this sector is characterized by the highest K^{+} mean concentration (8.1 mg/L) and the lowest Ca^{2+} average content (163.4 mg/L) (Table A.1). Most samples from Sector B reveal SO_4^{2-}-Ca^{2+} facies, except for sample G1 (spring), whose chemical composition is of HCO_3^{-}-Ca^{2+} type, and sample G2, of HCO_3^{-}-SO_4^{2-}-Ca^{2+} type. Regarding sector C, the only

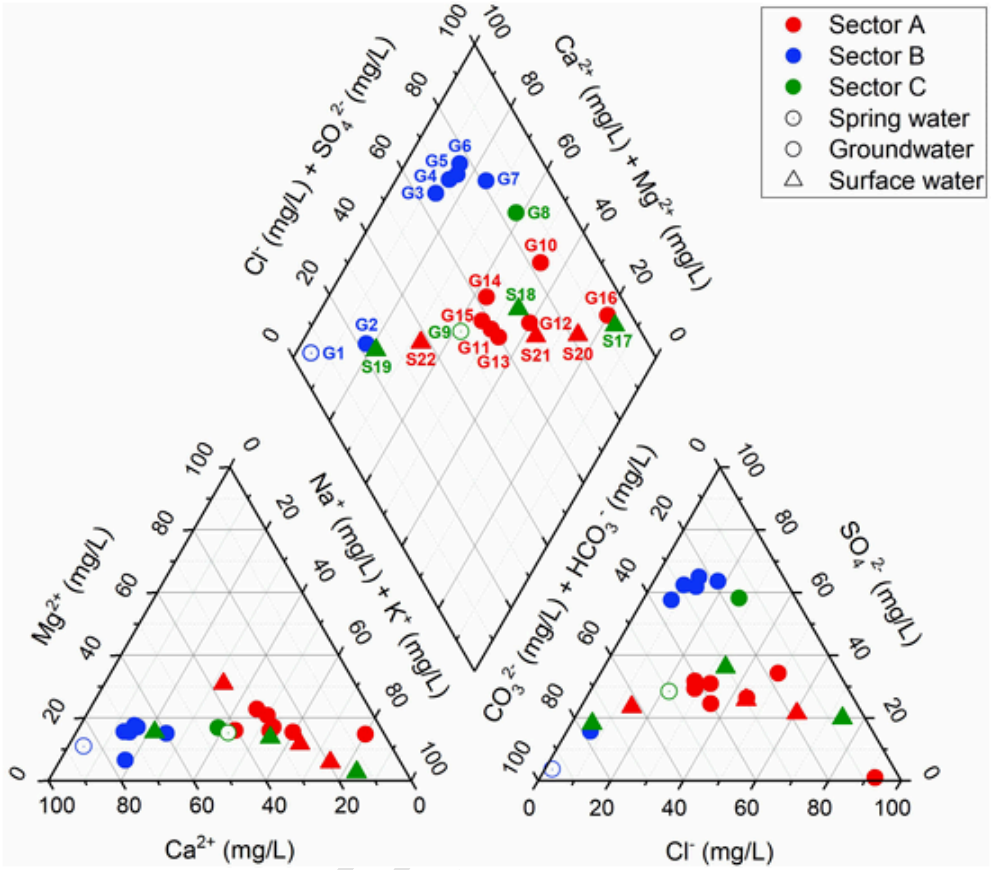

Fig. 4. Piper diagram of monitored spring waters, groundwater and surface waters in the three target areas (sectors A, B and C) of the Guadalhorce River basin.

groundwater sample collected, G8, is of SO_4^{2-}-Ca^{2+} type and showed the highest Sr^{2+} concentration (6.2 mg/L; Table A.1). Sample G9 (spring) is of HCO_3^--SO_4^{2-}-Ca^{2+} type and surface water in dams S17 and S19 are of Cl^--Na^+ and HCO_3^--Ca^{2+} types, respectively (S18 showing an intermediate chemical composition).

Threshold values for SO_4^{2-} and NO_3^- in groundwater (250 and 50 mg/L, respectively; EU, 2006) were exceeded in most of the groundwater samples of all sectors. These anion maximum values (923.5 and 491.8 mg/L for SO_4^{2-} and NO_3^-, respectively) were observed in groundwater sample G8 in sector C. Spring and surface water samples were characterized by low NO_3^- contents in the three target areas. The highest SO_4^{2-} concentration in surface water was observed in sample S17 in sector C (collected from the Guadalhorce dam) (Table A.1).

4.2. Isotopic characterization

4.2.1. Hydrogen and oxygen isotope variations

Results of water stable isotopes determinations were plotted on a conventional δ^2H-H_2O vs. $\delta^{18}O$-H_2O diagram (Fig. 5.1), together with the Global Meteoric Water Line (GMWL) (Craig, 1961), the trendlines of groundwater and surface waters and the LMWL, all of which were obtained through orthogonal regression. The LMWL is given by the equation: δ^2H ‰ = (6.57 ± 0.14) $\delta^{18}O$ + (5.23 ± 0.68) ‰ (R^2 = 0.87) (Barberá Fornell et al., 2018; IAEA, 2017). For the Gibraltar rainwater, the weighted isotopic composition ranges from −78.0 to 8.0‰, with a mean value of −25.8‰ for δ^2H-H_2O, and from −11.49 to 0.97‰, with an average value of −4.76‰ for $\delta^{18}O$-H_2O.

As can be observed in Fig. 5.1, most water sampling points fall along the GMWL and the LMWL (in the case of samples from sector A) lines. Waters from the upper sub-basin (sectors B and C) are generally more depleted in δ^2H-H_2O vs. $\delta^{18}O$-H_2O than waters from the lower one (sector A) (Table A.2). The isotopic composition of sector A waters varies from −35.6 to −23.8‰, with an average value of −29.3‰ for δ^2H-H_2O, and from −5.98 to −3.21‰, with a mean value of −4.61‰ for $\delta^{18}O$-H_2O. An evaporation water line is formed by water samples from this area. This trendline equation is equal to: δ^2H ‰ = (4.10 ± 0.22) $\delta^{18}O$ + (−10.37 ± 1.04) ‰ (R^2 = 0.97). On the other hand, the isotopic content of waters in sector B range between −43.4 and − 36.7‰, with an average value of −38.4‰ for δ^2H-H_2O, and between −7.46 and − 5.55‰, with a mean value of −6.00‰ for $\delta^{18}O$-H_2O. These waters also fall along an evaporation line, whose equation is: δ^2H ‰ = (3.48 ± 0.19) $\delta^{18}O$ + (−17.53 ± 1.17) ‰ (R^2 = 0.98). The two spring samples located in sectors B and C show the more depleted isotope content, while the dam samples (specially samples S17 and S18) from sector C have more enriched water isotope concentrations.

4.2.2. Carbon isotope variations in DIC and $CO_{2(g)}$ and strontium isotope ratio

$\delta^{13}C$-DIC and $\delta^{13}C$-$CO_{2(g)}$ values for waters in sector A vary between −17.8 and −9.3‰, with a mean value of −13.8‰, and between −25.3 and −16.8‰, with an average value of −21.3‰; respectively. In sector B, values range from −14.2 to −12.3‰, with an mean value of −13.1‰ for $\delta^{13}C$-DIC, and from −21.9 to −15.6‰, with an average value of −20.4‰ for $\delta^{13}C$-$CO_{2(g)}$. In sector C, $\delta^{13}C$-DIC and $\delta^{13}C$-$CO_{2(g)}$ values vary between −13.7 and −7.1‰, with a mean value of −9.5‰, and between −21.4 and −14.1‰, with an average value of −16.8‰, respectively. Minimum values (−17.8‰ for $\delta^{13}C$-DIC and −25.3‰ for $\delta^{13}C$-$CO_{2(g)}$) were recorded in sample G16, where also the minimum value of DIC (74.9 mg/L) was measured (Table A.1). Maximum values (−7.1‰ for $\delta^{13}C$-DIC and −14.1‰ for $\delta^{13}C$- $CO_{2(g)}$) were recorded in dam sample S18 (Guadalteba reservoir).

For the $^{87}Sr/^{86}Sr$ ratios determined in waters of the study area, values vary between 0.708263 and 0.709892 in sector A, between

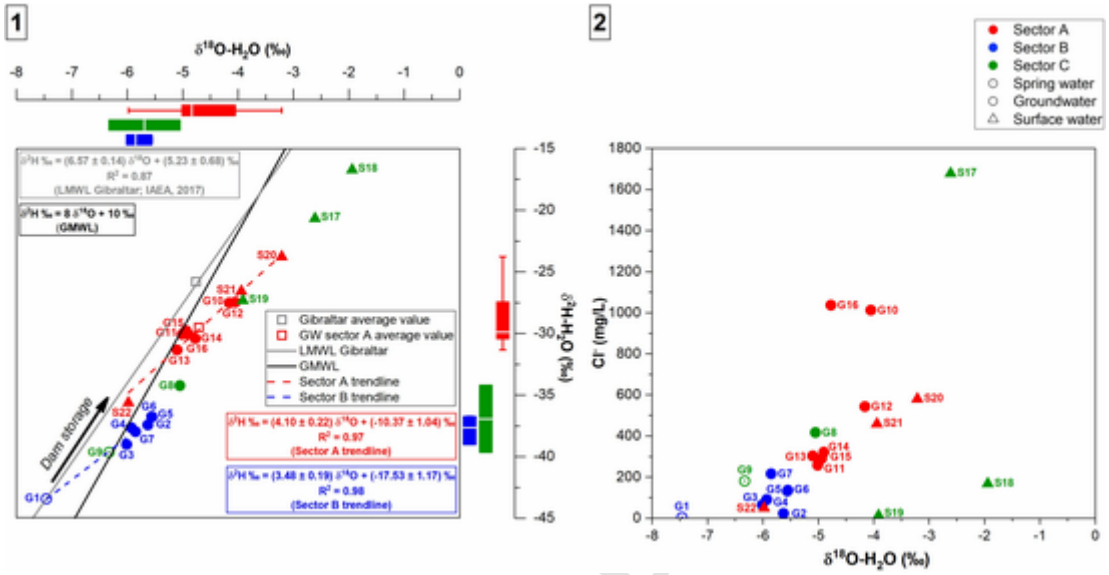

Fig. 5. (1): Water stable isotope composition (δ^2H-H_2O (‰) vs. δ^{18}O-H_2O (‰)) of spring waters, groundwater and surface waters in the three target areas (sectors A, B and C) of the Guadalhorce River basin (the dam system isotope composition was not considered when performing the box plots of sector C); (2): Relation of Cl^- (mg/L) and δ^{18}O-H_2O (‰) of monitored water in sectors A, B and C.

0.708024 and 0.708528 in sector B and between 0.708107 and 0.708358 in sector C (Table A.2).

5. Discussion

5.1. Hydrochemical characterization and water isotope variations

In the GRB, there is a close relationship between the use of developed land, the hydrogeological characteristics and the distinct types of water chemistry (Figs. 2, 4). Mixed types of waters, together with high EC values and SO_4^{2-} and NO_3^- concentrations, were observed in most of the samples of the target sectors (Table A.1). This fact indicates that water composition results from different processes: rock-water interaction, especially in the upper sub-basin, and water chemistry alteration by anthropogenic activities, principally in the lower one (Llamas-Dios et al., 2020, 2021). The natural contribution of the evaporitic basement to groundwater in the upper sub-basin ranges between around 70 to 85% of the total dissolved SO_4^{2-} (Urresti-Estala et al., 2015). This is reflected by the chemical composition of groundwater in sectors B (samples G3-G7) and C (sample G8).

While the composition of the spring samples collected in sector B (G1) and C (G9) supports their carbonate nature, the Triassic sediment fingerprint is evidenced by the chemical content of this last sampling point. Regarding sector B, this gypsum signal is less marked in sample G2, which displays low SO_4^{2-} content (56.2 mg/L; Table A.1) unlike the other samples, where SO_4^{2-} concentrations exceed threshold values, indicating a source from sewage discharge. This is because many locations throughout the basin lack wastewater treatment plants and are not connected to the sewer system. All groundwater samples from this sector show NO_3^- concentrations above the recommended limit. These were collected in areas with herbaceous crops like wheat, barley, legumes or tubers, where NH_4^+ fertilizers (mainly $(NH_4)_2SO_4$ and $NH_4NO_3SO_4$) are very common and are the source of this anion in groundwater. The presence of NO_3^- in sample G8 of sector C, with a value also exceeding the threshold limit, is due to manure, given the intensive pig farming and pig slurry irrigation typical of this zone (Urresti-Estala et al., 2015) (Fig. 2).

Variability in the chemical composition of surface waters in sector C (dams) (Fig. 4) is a consequence of the hydrological influence of two very different areas. The higher dissolved mineral content of the Guadalhorce dam sample (S17), dominated by Na^+, Cl^- and SO_4^{2-} ions and with the highest EC value (Table A.1), is due to its location in an endorheic zone and to the Meliones spring contribution from the evaporitic aquifer (Carrasco-Cantos et al., 2007). The dominance of Ca^{2+} and HCO_3^- ions and a low EC value (Table A.1) in the Conde de Guadalhorce dam sampling point (S19) comes from the dissolution of calcite and dolomite of the Ronda Mountain Range. The intermediate composition of the Guadalteba dam sample (S18) is due to its drainage basin also lying in the Antequera endorheic area, coupled with an accumulation of saline water in its bottom originating from the Guadalhorce dam (Armengol et al., 1990).

The effect of surface water flowing from dams into the waters of sector A is reflected by their chemical and isotopic composition. As can be seen in Fig. 5.1, most groundwater samples of the target sectors plot along the GMWL, showing a source of aquifer recharge from rainwater (Barberá Fornell et al., 2018), which represents an end member; evaporation during dam storage generates δ^2H-H_2O and δ^{18}O-H_2O enrichment, revealing a second end member. This acts as a groundwater and surface water source in the lower sub-basin. For this reason, surface water sampling point S20, which receives water directly from these reservoirs to meet agricultural demand, shows the highest evaporation value and, therefore, a composition dominated by Na^+, Cl^- and SO_4^{2-} ions (Table A.1; Fig. 4). Water use for irrigation infiltrates into the aquifer and is evaporated and salinized, and is then pumped back to the surface and further reused. The effect of these return flows and continuous pumping is mainly reflected by the high Cl^- content and δ^{18}O-H_2O values, which are characteristic of groundwater samples G10 and G12, as opposed to the values that would be typically found in the direction of flow. The chemical (high Na^+, Cl^- and SO_4^{2-} content; Table A.1; Fig. 4) and water isotope composition of surface sample S21 indicate the existence of groundwater-surface water exchange processes (Durán Valsero, 2007; Urresti-Estala et al., 2015; Llamas-Dios et al., 2020).

Surface water sample S22 (sector A; Fig. 1) is characterized by a distinct chemical composition (predominance of HCO_3^- and Mg^{2+} ions and low SO_4^{2-} concentration; Table A.1; Fig. 4) and isotopic fingerprint, having the most depleted water isotope content in this sector (Fig. 5). This is due to the Grande River, before its confluence with the Guadalhorce River, receiving waters from rivers draining the northern edge of the carbonate Sierra Blanca massif (Fig. 1), resulting in the prevalence of the calcite and dolomite dissolution fingerprint. On the

other hand, the evaporation water line formed by water samples from sector B (Fig. 5.1) is also potentially attributed to irrigation return flows (Vadillo-Pérez et al., 2019). In this area, sample G1 shows the most depleted δ^2H-H_2O and $\delta^{18}O$-H_2O content as a consequence of this spring recharge source from precipitation at the highest altitude (altitude effect).

Groundwater sample G16, the nearest to the coastline (sector A; Fig. 1), shows a predominance of Cl^- and Na^+ ions in its composition (Table A.1; Fig. 4), suggesting seawater influence (Luque Espinar et al., 2003; Urresti-Estala et al., 2016; Llamas-Dios et al., 2020, 2021). The inverse model obtained validated the plausibility of this hydrochemical observation and provided some insights on the processes affecting the major ion composition and isotopic fractionation. The strong increase of the Cl^- content toward sample G16 is explained by the mixing of waters, seawater having about 19 g/L of Cl^-. Sample G13 was used as the other extreme member representative of non-salinized groundwater. As can be seen in Table 1, ion contents increase (and consequently ionic strength) and carbonates precipitate. Seawater-freshwater mixing produces an increase in SI_{cal} and SI_{str} values (Table A.1), and this leads to the precipitation of calcite (and consequently $CO_{2(atm)}$ outgassing) and strontianite (in a smaller proportion). K^+ is removed through K-montmorillonite formation. However, it is possible that K adsorption occurs, but this process cannot be simulated using the Netpath code. Cation exchange explains an important proportion of the composition, being noticeable the sense of the Ca/Na exchange, with Na^+ adsorption and Ca^{2+} release, which is typical of seawater intrusion processes (Martínez and Bocanegra, 2002). Mg^{2+} exchange is a secondary process, with this ion being adsorbed and Na^+ being released.

Additionally, sample G16 is characterized by a very low SO_4^{2-} content (11.5 mg/L; Table A.1), the source of this anion being attributed to fertilizer input and untreated wastewater (Urresti-Estala et al., 2016). In a seawater/freshwater mixing context, water becomes less oxidant due to a change in oxidation-reduction conditions, as evidenced by the highest pH and the lowest DO values of sample G16. In this reducing environment, the Fe-S formation (Nadler et al., 1980; Bosch and Custodio, 1993) is one of the processes that can control the decline in the SO_4^{2-} concentration toward sample G16. Fe-S precipitation was an imposed condition at the moment of modelling, considering the existence of disseminated pyrite in the Paleozoic shales of the Malaguide Complex tectonic unit (Galvez and Orozco, 1979; Herbig, 1985) (Table 1). As regards isotopic data, when comparing the carbon and strontium isotopes contents of this final water G16 calculated by the Rayleigh model (−13.5‰ and 0.7088 for $\delta^{13}C$-DIC and $^{87}Sr/^{86}Sr$, respectively) with those observed (−17.8‰ and 0.7093 for $\delta^{13}C$-DIC and $^{87}Sr/^{86}Sr$, respectively; Table A.2. See detailed discussion in Section 5.2), it can be seen differences between them (slighter in the case of $^{87}Sr/^{86}Sr$). These may be a consequence of the mass balance model uncertainties when calculating the carbonates precipitation. Lastly, although the chemical composition of sample G16 suggests seawater intrusion, its water isotope content (−30.4‰ for δ^2H-H_2O and −4.77‰ for $\delta^{18}O$-H_2O; Table A.2) approaches that of the Gibraltar rainwater (weighted mean values: −25.8‰ for δ^2H-H_2O and −4.76‰ for $\delta^{18}O$-H_2O) (Fig. 5.1). This is because of a negligible contribution of seawater to groundwater (calculated value of 4%) and a source of aquifer recharge from precipitation.

Except for sample G16, groundwater sampling points of sector A show high concentrations of SO_4^{2-} (Table A.1), most of which exceed the threshold value. This is the opposite of what would be expected in these samples as they approach the coastline, due to the absence of the Triassic basement and the dilution effect as a result of water contribution from tributary rivers in the lower reach of the Guadalhorce River. Urresti-Estala et al. (2015) have concluded that the main aquifer from where these samples were collected receives only around 10–30% of the total SO_4^{2-} derived from natural inputs, which means that, input from fertilizers represents over 80% in this lower sub-basin. Likewise, these authors have also demonstrated that the NO_3^- presence in groundwater of this sector comes from mixing processes between NH_4^+ fertilizers and other pollution sources like manure (both in relation to the presence of citric crops) or sewage from residential areas (Fig. 2). Finally, NO_3^- concentrations of springs (sectors B and C) and surface waters (sectors A and C) sampling points did not reflect the existence of the widespread nitrate pollution problem affecting groundwater samples throughout the three study areas.

5.2. Carbon isotope variations in DIC and $CO_{2(g)}$ and strontium isotope ratio

The carbon isotope of DIC and $CO_{2(g)}$ and $^{87}Sr/^{86}Sr$ results have supported the previously proposed results (Fig. 3). In Fig. 6, waters from the target sectors were represented in a $\delta^{13}C$-DIC vs. DIC diagram, assuming that: 1) the current atmospheric CO_2 ($CO_{2(atm)}$) has $\delta^{13}C$-DIC ~−8.4‰ (Graven et al., 2017); 2) the biogenic soil CO_2 ($CO_{2(soil)}$) $\delta^{13}C$-DIC is within the range of −25.0 to −23.0‰ in soils hosting Calvin or C3 vegetation (Clark and Fritz, 1997; Mook, 2002), as is the case of the GRB upper (herbaceous crops) and lower (citric crops) sub-basins; 3) the $CO_{2(atm)}$ incorporation into waters mainly takes place in an open system (unconfined nature of the Quaternary aquifer) and at pH values under 8 in almost all water sampling points, in which most of DIC occurs as HCO_3^- (Table A.1); and 4) the $\delta^{13}C$-DIC is close to 0‰ for carbonate minerals (Clark and Fritz, 1997; Mook, 2002).

Table 1
Reactant phases values in millimoles per litre (mmol/L) obtained as result in NetpathXL code output for the sector A of the GRB (southern sector). (−): precipitated/outgassed/Ca^{2+} and/or Mg^{2+} released and Na^+ adsorbed; (+): dissolved/Ca^{2+} and/or Mg^{2+} adsorbed and Na^+ released.

Mineral phase	Model	
	IS[a]	***FS***[b]
	Mixture seawater: sample G13 (0.04:0:96)	sample G16
Calcite	−4.0	
$CO_{2(atm)}$	−0.8	
Fe-S	−3.1[c]	
K-montorillonite	−0.8	
Ca/Na exchange	−1.6	
Mg/Na exchange	0.4	
Strontianite	−0.003	

[a] ***IS***: initial solution.
[b] ***FS***: final solution.
[c] Precipitation as an imposed condition.

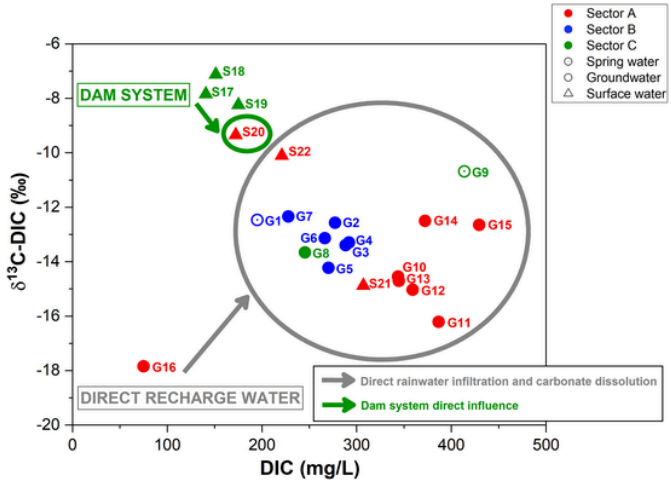

Fig. 6. $\delta^{13}C$-DIC (‰) vs. DIC (mg/L) graph for spring waters, groundwater and surface waters of the three target areas (sectors A, B and C) of the Guadalhorce River basin.

Distinct types of waters could be differentiated (Fig. 6). One is groundwater from sample G16, with the lowest DIC, δ^{13}C-DIC and δ^{13}C-$CO_{2(g)}$ contents (74.9 mg/L, −17.8‰ and −25.3‰, respectively: Tables A.1 and A.2), showing a $CO_{2(soil)}$ dominance and revealing the direct rainwater recharge as an end member. On the other hand, when rainwater reacts with carbonate materials in an open system, $CO_{2(soil)}$ incorporation into water occurs, increasing the δ^{13}C-DIC, δ^{13}C-$CO_{2(g)}$ and DIC values due to the dissolution of these geological materials present in the area. Consequently, the relatively high (>200 mg/L) DIC values, the δ^{13}C-DIC (varying between −16.2 and −10.7‰) and the δ^{13}C-$CO_{2(g)}$ (ranging from −24.3 to −15.6‰) (Tables A.1 and A.2) released into groundwater samples of the upper and lower sub-basins is a mixture between the isotopic signature of the $CO_{2(soil)}$ and that of carbonates. The δ^{13}C-$CO_{2(g)}$ composition reveals the dominant processes occurring in the unsaturated zone, which are later translated to the shallow aquifer. The dominance of the CO_2 from the C3 plants, but with some enrichment resulting from carbonates equilibrium, is evidenced. The DIC, δ^{13}C-DIC and δ^{13}C-$CO_{2(g)}$ contents (307.1 mg/L, −14.9‰ and −22.1‰, respectively; Tables A.1 and A.2) of surface water sampling point S21 sustain the existence of groundwater-surface water exchange processes. In addition, carbonate weathering processes (calcite and dolomite dissolution) control the DIC, δ^{13}C-DIC and δ^{13}C-$CO_{2(g)}$ values characteristic of surface sample S22 (221.0 mg/L, −10.1‰ and −16.8‰, respectively; Tables A.1 and A.2). The second end member, the dam system, is characterized by a lower DIC content (average value of 155.8 mg/L) and heavier δ^{13}C-DIC and δ^{13}C-$CO_{2(g)}$ values (mean values of −7.7‰ and −14.7‰, respectively). This evidences the isotopic exchange with the $CO_{2(atm)}$. In the northern part of sector A, surface water sample S20 reflects the direct influence from these reservoirs on its composition (172.4 mg/L for DIC, −9.3‰ for δ^{13}C-DIC and −16.8‰ for δ^{13}C-$CO_{2(g)}$; Tables A.1 and A.2).

As shown in Fig. 7, the average δ^{18}O-H_2O values of groundwater samples from the GRB lower sub-basin (−4.70‰) and precipitation in the Gibraltar region (−4.76‰) (Fig. 5.1) are similar, evidencing the aquifer recharge source from rainwater infiltration. A δ^{18}O-H_2O mean value of −7.8‰ can be assumed for rainwater in the recharge zones of sectors B and C. This value was calculated considering a depletion of −0.5‰ per 100-rise in altitude (Clark and Fritz, 1997) and the 595 m difference (DEM in Fig. 1) between the plain zone (weighted mean δ^{18}O-H_2O value of −4.76‰ in the Gibraltar rainfall station) and the upper sub-basin's mountain areas (the average altitude value of the two springs sampled was considered). The more enriched δ^{18}O-H_2O and δ^{13}C-DIC content of the dams sampling points and sample S20 evidence the occurrence of $CO_{2(atm)}$ outgassing and the evaporation process, and the direct influence from these reservoirs on this river water composition, respectively. In addition, the composition of groundwater samples G10 and G12 reflects the irrigation return effect, while that of sample S21 shows the existence of groundwater-surface water exchange processes. Lastly, the distinct composition of sample S22 evidences the carbonate material dissolution fingerprint characteristic of its tributary rivers.

Regarding strontium concentrations and isotopes (Fig. 8.1), groundwater and surface water samples from the upper sub-basin are characterized by the highest mean content of Sr^{2+} (3.0 and 2.4 mg/L for sectors B and C, respectively; Table A.1), which is consistent with waters flowing through mainly evaporites (gypsum) bedrocks in an area of relatively low rainfall (Palmer and Emond, 1989; Soler et al., 2002), as Sr^{2+} readily substitutes in Ca-bearing rocks and minerals. Sr^{2+} is released to surface water and groundwater primarily through processes of weathering, and studies have shown this cation to be highly soluble and mobile (Middelburg et al., 1988; Borg and Banner, 1996; Banner, 2004). Evaporites and carbonates are potential sources of Sr^{2+} or are likely associated with Sr^{2+} minerals (celestite, strontianite) (Hem, 1992). Evaporites can incorporate up to 3500 mg/L Sr^{2+} into their lattices, while this concentration is averaging ~600 mg/L in carbonate materials (Kinsman, 1969; Dean, 1978; Hem, 1992). Waters samples in these sectors show the lowest $^{87}Sr/^{86}Sr$ values (between 0.708024 and 0.708528; Table A.2), which allow corroborating the contribution from

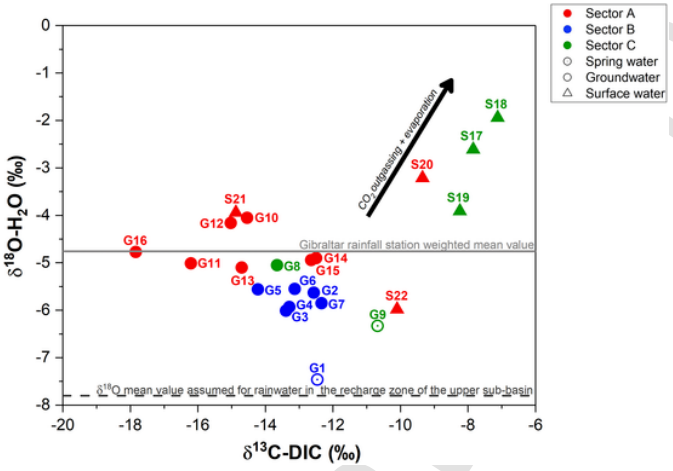

Fig. 7. δ^{18}O-H_2O (‰) vs. δ^{13}C-DIC (‰) graph for spring waters, groundwater and surface waters of the three target areas (sectors A, B and C) of the Guadalhorce River basin.

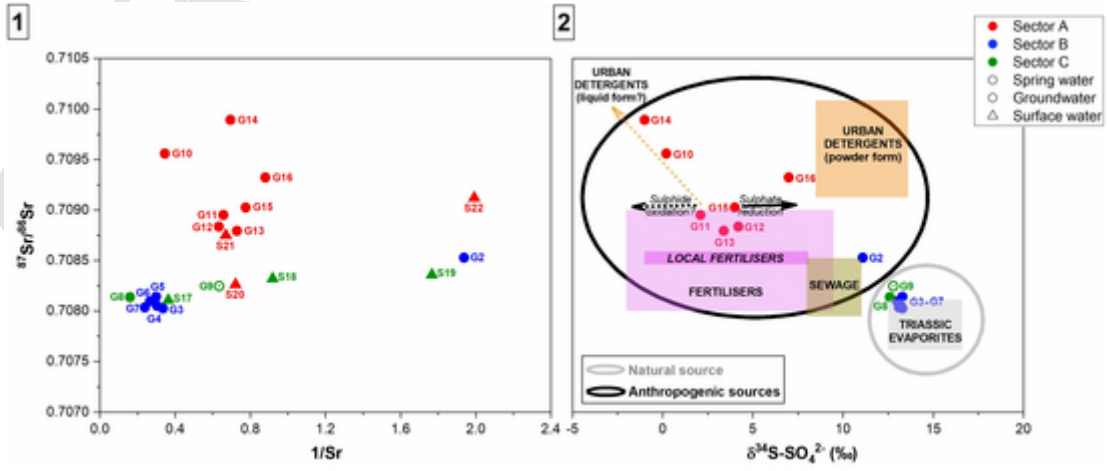

Fig. 8. (1): $^{87}Sr/^{86}Sr$ vs. 1/Sr diagram for spring waters, groundwater and surface waters and (2): $^{87}Sr/^{86}Sr$ vs. δ^{34}S-SO_4^{2-} (‰) (Urresti-Estala et al., 2015) graph for spring waters and groundwater of the three target areas (sectors A, B and C) of the Guadalhorce River basin.

the Triassic evaporites (between 0.707615 and 0.708114; Ortí et al., 2014) and carbonates (~0.708; Faure, 1986) to their composition.

Specifically, the higher Sr^{2+} contents and the strontium isotope values of groundwater sampling points of sector B (except for sample G2), groundwater sample G8 and dam sampling point S17, the last two located in sector C (Tables A.1 and A.2), evidence the evaporitic material signature domain. As explained previously, this gypsum signal is less marked in sample G2 because of the influence of sewage in its composition, so the low Sr^{2+} concentration of this sampling point is reflecting the carbonate dissolution predominance (SI_{cal}: −0.9; Table A.1) ($^{87}Sr/^{86}Sr$ value explained below). On the other hand, the lower Sr^{2+} content and the $^{87}Sr/^{86}Sr$ value characteristic of dam sampling point S19 (sector C) (Tables A.1 and A.2) are consistent with a carbonate dissolution fingerprint in its composition. The latter is also applicable to spring sample G1 (sector B), considering its $^{87}Sr/^{86}Sr$ value (Table A.2) and assuming a low Sr^{2+} content for this sampling point (no Sr^{2+} analysis is available for this sample). A mixture between the contribution of the Triassic basement and carbonates is corroborated by the intermediate Sr^{2+} content and the $^{87}Sr/^{86}Sr$ ratio of spring sample G9 and dam sampling point S18 of sector C (Tables A.1 and A.2; Fig. 8.1).

Conversely, waters from the lower sub-basin have the lowest average Sr^{2+} content (1.5 mg/L; Table A.1), which is consistent with the lesser contribution/absence of the Triassic basement in the northern and southern part of this sector, respectively. The presence of calcareous sediments in the Quaternary aquifer of sector A explains the main source of Ca^{2+} and also Sr^{2+}. The lowest Ca^{2+} average content and the highest K^+ mean concentration characteristic of groundwater in this sub-basin (Table A.1) could be evidencing the occurrence of silicates (present in the alluvial sediments) weathering and ionic exchange processes.

Sample S22 presents the lowest Sr^{2+} concentration observed in surface water (Table A.1), which is in agreement with the calcite and dolomite dissolution contribution in its composition ($^{87}Sr/^{86}Sr$ value explained below). Except for river water sample S20, whose strontium concentration and isotope composition reflect the evaporite signature domain due to the direct influence of the dams, the presence of the highest $^{87}Sr/^{86}Sr$ content (between 0.708748 and 0.709892; Table A.2) in all groundwater and surface waters samples S21 and S22 of sector A cannot be explained with natural sources. Considering the land use developed in this area (Fig. 2) and the one mentioned in previous paragraphs, a mixing of anthropogenic sources is required to explain this data (Antich et al., 2000; Soler et al., 2002). This is also applicable to groundwater sample G2 (sector B) (Fig. 8.1).

Comparing $^{87}Sr/^{86}Sr$ vs. $\delta^{34}S\text{-}SO_4^{2-}$ values for groundwater samples of the GRB (Fig. 8.2; Table A.2), the latter ones taken from the work of Urresti-Estala et al. (2015) and considered as representative of the isotopic signal of SO_4^{2-} in the study area (samples also collected at times not corresponding with the wet season), it can be proved that two main end members can be differentiated: the Triassic evaporites, on the one hand, and the anthropogenic activities, on the other. Evaporitic basement values were taken from Ortí et al. (2014), with typical ranges for fertilizers (and local fertilizers: $(NH_4)_2SO_4$ and $NH_4NO_3SO_4$), mixed urban and industrial wastes and urban detergents (in powder form) taken from Antich et al. (2000) and Vitòria et al. (2004, 2005). Groundwater samples from sectors B (except sample G2) and C show a signal lying close to the area defined by the isotopic range of the Triassic evaporites, evidencing the strong influence of this natural source in their composition. However, groundwater sample G2 is reflecting the influence of sewage.

For sector A, the composition of samples G11, G12, G13 and G15 reveals a contribution from fertilizers (Fig. 8.2). According to the $^{87}Sr/^{86}Sr$ ratios found in river water samples S21 and S22 (Fig. 8.1), the influence of fertilizers on their composition can also be assumed. In this area, sampling points G10, G14 and G16 are characterized by $^{87}Sr/^{86}Sr$ ratios higher than those of fertilizers (Fig. 8.2). In the case of sample G16, its isotope composition is attributed to the contribution of fertilizers and also of the powder detergents used in the region. Its more enriched $\delta^{34}S\text{-}SO_4^{2-}$ content with respect to samples G11, G12, G13 and G15 is due to the occurrence of the sulphate reduction process mentioned previously.

Conversely, samples G10 and G14 show the most depleted $\delta^{34}S\text{-}SO_4^{2-}$ content (Fig. 8.2), which could be linked to sulphide oxidation processes (Urresti-Estala et al., 2015). However, these $\delta^{34}S\text{-}SO_4^{2-}$ content and the highest $^{87}Sr/^{86}Sr$ ratios characteristic of these sampling points could indicate the existence of another anthropogenic source, which could be the influence of urban detergents whose raw materials have origins different from those used to manufacture powder detergents, as is the case of liquid detergents, providing different isotopic signatures as a result. In Spain, sodium sulphates (glauberite) used in the manufacture of powder detergents have been replaced by other components (like sodium laureth sulphate, among others) for the production of liquid detergents (del Cura and Delgado, 1992). Although the $\delta^{34}S\text{-}SO_4^{2-}$ signature of detergents in liquid form has not been studied in Spain, as neither has the $^{87}Sr/^{86}Sr$ fingerprint of this type of detergents, neither in this country nor in other regions of the world, some contributions related to the $\delta^{34}S\text{-}SO_4^{2-}$ composition of liquid detergents in Asian cities exist (Hosono et al., 2007; Zhang et al., 2015; Wang and Zhang, 2019). Hosono et al. (2007) have demonstrated that liquid detergents clearly show lower $\delta^{34}S\text{-}SO_4^{2-}$ values (−3.2 to −2.1‰) than powder detergents (+4.0 to +25.8‰). According to these authors, this could be attributed to different sources of the raw materials providing sulfur, that is, in the case of Japan, crude oils mainly imported from the Middle East with variable $\delta^{34}S\text{-}SO_4^{2-}$ content (−5.0 to +10‰; Grinenko and Grinenko, 1991; Pankina, 1991). Therefore, it is evident that when raw materials used for manufacturing detergents have different origins, the isotopic fingerprint is also different. Accordingly, an isotopic gap between the liquid and powder detergents used in Spain could be assumed.

6. Conclusions

This multi-tracer study allowed taking a step further in accurately determining contamination sources and processes in the Guadalhorce River Basin. DIC, stable isotopes of water and carbon in DIC revealed the existence of two groundwater and surface water recharge end members. Direct rainwater infiltrated into the upper and lower detritic aquifers of the sub-basins, with DIC values ranging from ~70 to 400 mg/L, the more isotopically depleted water ($\delta^{18}O\text{-}H_2O$ from ~−7.00 to 5.00‰), and $\delta^{13}C$-DIC (from ~−18 to −10‰) and $\delta^{13}C\text{-}CO_{2(g)}$ (from ~−25 to −16‰) in the range of $CO_{2(soil)}$ interacting with carbonates. The other end member is the dam system, with intermediate DIC content (mean value of 155.8 mg/L), isotopically enriched ($\delta^{18}O\text{-}H_2O$ average value of −2.82‰) and high $\delta^{13}C$-DIC and $\delta^{13}C\text{-}CO_{2(g)}$ (mean values of −7.7 and −14.7‰, respectively).

The difference between the strontium isotope composition of natural and anthropogenic sources is a powerful additional tool when other isotopes used as water pollution tracers can no longer discriminate between closely overlapping results. $^{87}Sr/^{86}Sr$ data support the previously results arrived to in relation to contamination sources in the GRB waters. Triassic evaporites generally control the natural $^{87}Sr/^{86}Sr$ composition in waters of the upper sub-basin. Only one groundwater sample reflects the influence of a human organic source (sewage) in its composition. On the other hand, mixing of human inorganic (fertilizers and detergents) strontium sources is required to explain the $^{87}Sr/^{86}Sr$ content of the lower sub-basin waters. Discriminating the use of domestic detergents as another anthropogenic source of strontium and sulphate in water through the analysis of the $^{87}Sr/^{86}Sr$ ratios and $\delta^{34}S\text{-}SO_4^{2-}$ values previously determined in the basin is a novel finding in this research. The isotopic fingerprint analysis of the different types of

synthetic detergents would allow for a better understanding of the role these anthropogenic sources play in water pollution in the GRB.

The results obtained highlight the importance in the use of isotopes as pollutant tracers. The conclusions arrived at are significant in terms of water resource management in the study site and can be extrapolated to other highly anthropized basins.

Funding

This work was partially supported by the International Atomic Energy Agency (IAEA, Vienna, Austria) through the Project RLA7018: "Improving Knowledge of Groundwater Resources to Contribute to their Protection, Integrated Management and Governance (ARCAL CXXXV)".

CRediT authorship contribution statement

M. Glok-Galli: Conceptualization, Formal analysis, Funding acquisition, Investigation, Visualization, Writing-original draft, Writing-review & editing; **I. Vadillo-Pérez**: Conceptualization, Data curation, Funding acquisition, Investigation, Methodology, Project administration, Resources, Supervision, Writing-review & editing; **Jiménez-Gavilán, P.**: Conceptualization, Data curation, Investigation, Methodology, Supervision; **Ojeda, L.**: Conceptualization, Investigation, Methodology, Resources, Validation; **Urresti-Estala, B.**: Conceptualization, Investigation, Resources; **Martínez, D.E.**: Formal analysis, Visualization.

Declaration of competing interest

The authors declare that they have no known competing financial interests or personal relationships that could have appeared to influence the work reported in this paper.

Acknowledgments

The authors would like to thank the financial support of the International Atomic Energy Agency (IAEA, Vienna, Austria) through the Project RLA7018: "Improving Knowledge of Groundwater Resources to Contribute to their Protection, Integrated Management and Governance (ARCAL CXXXV)", from which a training scholarship was awarded to Dr. M. Glok-Galli (Workplace: University of Malaga (Spain); Supervisor: I. Vadillo-Pérez) and which made conducting this project possible. This article is also a contribution to the Research Group of the "Junta de Andalucía" (Group of Hydrogeology, RNM-308). We are grateful to technical translation specialists GeoTranslations for proofreading the English version. We would also like to thank Prof. Dr. Jurgen Mahlknecht, the Associate Editor, and the anonymous reviewers, who largely contributed to the improvement of the manuscript.

Appendix A. Supplementary data

Supplementary data to this article can be found online at https://doi.org/10.1016/j.scitotenv.2022.154424.

References

Antich, N., Canals, A., Soler, A., Darbyshire, D.P.F., Spiro, B.F., 2000. The isotope composition of dissolved strontium as a tracer of pollution in the Llobregat River, northeast Spain. In: Dassargues, A. (Ed.), Tracers and Modelling in Hydrogeology. Proceedings of die TraM'2000 Conference held at Liège, Belgium, May 2000, 262. International Association of Hydrological Sciences, Oxfordshire, pp. 207–212.

Appelo, C.A.J., Postma, D., 2005. In: Geochemistry, Groundwater and Pollution, 2nd edition, A.A. Balkema Publishers, Leiden, The Netherlands a member of Taylor & Francis Group plc, p. 634 ISBN 04 1536 421 3.

Aravena, R., Robertson, W.D., 1998. Use of multiple isotope tracers to evaluate denitrification in ground water: study of nitrate from a large-flux septic system plume. Ground Water 36, 975–981.

Armengol, J., Catalán, J., Gabellone, N., Jaume, D., de Manuel, J., Martí, E., Morguí, J.A., Nolla, J., Peñuelas, J., Real, M., Riera, J.L., Sabater, S., Sabater, F., Toja, J., 1990. A comparative limnological study of the Guadalhorce reservoirs system (Malaga, S.E. Spain). Sci. Gerundensis 16 (2), 27–41.

Awaleh, M.O., Boschetti, T., Adaneh, A.E., Chirdon, M.A., Ahmed, M.M., Dabar, O.A., Soubaneh, Y.D., Egueh, N.M., Kawalieh, A.D., Kadieh, I.H., Chaheire, M., 2022. Origin of nitrate and sulfate sources in volcano-sedimentary aquifers of the East Africa rift system: an example of the Ali-Sabieh groundwater (Republic of Djibouti). Sci. Total Environ. 804, 150072. https://doi.org/10.1016/j.scitotenv.2021.150072.

Back, W., 1961. In: Techniques for Mapping Hydrochemical Facies. U.S. Geol. Survey Professional Paper, 424-D. pp. 380–382.

Banner, J.L., 2004. Radiogenic isotopes: systematics and applications to earth surface processes and chemical stratigraphy. Earth Sci. Rev. 65, 141–194. https://doi.org/10.1016/S0012-8252(03)00086-2.

Barberá Fornell, J.A., Andreo-Navarro, B., Abrisqueta Rangel, A.D., 2018. In: Caracterización hidrogeoquímica e isotópica de aguas minerales y termales de la provincia de Málaga. Communication, AIH Salamanca, p. 10.

Barbieri, M., Barberio, M.D., Banzato, F., Billi, A., Boschetti, T., Franchini, S., Gori, F., Petitta, M., 2021. Climate change and its effect on groundwater quality. Environ. Geochem. Health 1–12. https://doi.org/10.1007/s10653-021-01140-5.

BOJA, 2013. Orden de 2 de julio de 2013, por la que se dispone la publicación de las determinaciones de contenido normativo del Plan Hidrológico de la Demarcación Hidrográfica de las Cuencas Mediterráneas Andaluzas, aprobado por el Real Decreto 1331/2012, de 14 de septiembre. In: Boletín Oficial de la Junta de Andalucía, 138, pp. 67–289 (accessed on 15 July 2021) http://www.juntadeandalucia.es/boja/2013/138/16.

Borg, L.E., Banner, J.L., 1996. Neodymium and strontium isotopic constraints on soil sources in Barbados, West Indies. Geochem. Cosmochim. Acta 60, 4193–4206. https://doi.org/10.1016/S0016-7037(96)00252-9.

Bosch, X., Custodio, E., 1993. Dissolution processes in the freshwater–saltwater mixing zone in the Cala Jostel area (Vandellós, Tarragona). In: Proceedings of the XII salt water intrusion meeting, Barcelona, CIMNE-UPC. pp. 229–244.

Carrasco-Cantos, F., 1986. Contribution to the Knowledge of the Upper Basin of the Guadalhorce River: Physical Media. University of Granada, Granada, Spain (in Spanish). Ph.D. Thesis.

Carrasco-Cantos, F., Sánchez-García, D., Vadillo-Pérez, I., 2007. Sierra de Teba-Almargen-Campillos. In: Durán-Valsero, J.J., Andreo-Navarro, B. (Eds.), Atlas hidrogeológico de la provincia de Málaga, 1st ed., 2. Publishers: IGME, Madrid, Spain; Diputación Provincial de Málaga: Málaga, Spain, pp. 95–100.

Carrasco-Cantos, F., Sánchez-García, D., Vadillo-Pérez, I., Andreo, B., Martínez, C., Fernández, L., 2008. Application of the european water framework directive in a Western Mediterranean Basin (Malaga, Spain). Environ. Geol. 54, 575–585.

Cheng, L., Normandeau, C., Bowden, R., Doucett, R., Gallagher, B., Gillikin, D.P., Kumamoto, Y., McKay, J.L., Middlestead, P., Ninnemann, U., Nothaft, D., Dubinina, E.O., Quay, P., Reverdin, G., Shirai, K., Mørkved, P.T., Theiling, B.P., van Geldern, R., Wallace, D.W.R., 2019. An international intercomparison of stable carbon isotope composition measurements of dissolved inorganic carbon in seawater. Limnol. Oceanogr. Methods 17 (3), 200–209. https://doi.org/10.1002/lom3.10300.

Clark, I.D., 2015. In: Groundwater Geochemistry and Isotopes. CRC Press Taylor and Francis, p. 438.

Clark, I.D., Fritz, P., 1997. In: Environmental Isotopes in Hydrogeology. CRC, Boca Raton, p. 328.

Cook, P.G., Herczeg, A.L., 1999. In: Environmental Tracers in Subsurface Hydrology. Kluwer, Boston, MA, p. 529.

Craig, H., 1961. Standard for reporting concentrations of deuterium and oxygen-18 in natural waters. Science 133 (3467), 1833–1834.

Dean, W.E., 1978. Trace and minor elements in evaporites. In: Dean, W.E., Schreiber, B.C. (Eds.)Notes for a Short Course on Marine Evaporites, vol. 4. SEPM Short Course, pp. 86–105.

del Cura, M.Á.G., Delgado, S.O., 1992. El sulfato sódico natural en España: las salas sódicas de la Cuenca de Madrid. In: Recursos minerales de España (1229-1250). Consejo Superior de Investigaciones Científicas, CSIC (Superior Council of Scientific Investigations; SCSI).

Durán Valsero, J.J., 2007. Atlas hidrogeológico de la provincia de Málaga. Instituto Geológico y Minero de España, Diputación de Málaga.

EU, 2006. Groundwater directive, 2006, directive 2006/118/EC of the European parliament and the council of 12 December. In: Commission, E. (Ed.), On the protection of groundwater against pollution and deterioration, L 372. Official Journal of the European Union. pp. 19–25. https://eur-lex.europa.eu/legal-content/EN/TXT/PDF/?uri=CELEX:32006L0118&qid=1396858818203&from=EN.

Faure, G., 1986. Principles of Isotope Geology, 2nd ed. Wiley, Hoboken (NJ).

Galvez, R., Orozco, M., 1979. Strain determinations using deformed Radiolaria. Malaguide Complex, Southern Spain. Acta Geol. Hisp. 14, 129–134.

Geyh, M., 2000. Groundwater, vol. 4. Environmental isotopes in the hydrologic cycle. In: Mook, W.G. (Ed.), IHP-V Technical Documents in Hydrology N° 39. UNESCO, Paris, France, p. 196.

Glok-Galli, M., Martínez, D.E., Vadillo-Pérez, I., Silva Busso, A.A., Barredo, S.P., Quiroz Londoño, O.M., Trezza, M.A., 2020. Multi-isotope (δ^2H, $\delta^{18}O$, $\delta^{13}C$-TDIC, $\delta^{18}O$-TDIC, $^{87}Sr/^{86}Sr$) and hydrochemical study on fractured-karstic and detritic shallow aquifers in the Pampean region, Argentina. Groundwater Special Issue on Environmental Isotope Applications in the Latin America and Caribbean region (Groundwater Issue). Journal Isotopes of Environmental and Health Studies. 56 (5–6), 513–532. https://doi.org/10.1080/10256016.2020.1825412.

Gonfiantini, R., 1978. Standards for stable isotope measurements in natural compounds. Nature 271, 534–536.

Graven, H., Allison, C.E., Etheridge, D.M., Hammer, S., Keeling, R.F., Levin, I., Meijer,

H.A.J., Rubino, M., Tans, P.P., Trudinger, C.M., Vaughn, B.H., White, J.W.C., 2017. Compiled records of carbon isotopes in atmospheric CO2 for historical simulations in CMIP6. Geosci. Model Dev. 10 (12), 4405–4417. https://doi.org/10.5194/gmd-10-4405-2017.

Grinenko, L.N., Grinenko, V.A., 1991. Isotopic composition of sulphur in sulphide ores. In: Krouse, H.R., Grinenko, V.A. (Eds.), Stable Isotopes: Natural and Anthropogenic Sulphur in the Environment. Scope. pp. 87–91.

Hem, J.D., 1992. Study and Interpretation of the Chemical Characteristics of Natural Water. In: U.S. Geol. Surv. Water-Sup. Pap. 2254, third ed. https://doi.org/10.3133/wsp2254.

Herbig, H., 1985. An upper devonian limestone slide block near Marbella (Betic cordillera, southern Spain) and the paleographic relations between malaguides and menorca. Acta Geol. Hisp. 20, 155–178.

Hosono, T., Nakano, T., Igeta, A., Tayasu, I., Tanaka, T., Yachi, S., 2007. Impact of fertilizer on a small watershed of Lake Biwa: use of sulfur and strontium isotopes in environmental diagnosis. Sci. Total Environ. 384 (1–3), 342–354.

IAEA, 2017. IAEA-Wiser. https://nucleus.iaea.org/wiser/index.aspx (accessed on 10 August 2021).

Kendall, C., McDonnell, J.J., 1998. In: Isotope Tracers in catchment Hydrology. Elsevier Science B.V., Amsterdam, p. 839.

Kinsman, D.J., 1969. Interpretation of Sr2+ concentrations in carbonate minerals and rocks. J. Sediment. Petrol. 39, 486–508. https://doi.org/10.1306/74D71CB7-2B21-11D7-8648000102C1865D.

Linares, L., López-Arechavala, G., López-Geta, J.A., Campos-Rubio, J.C., 1995. Geometrical definition of the Pliocene-Quaternary aquifers of the Guadalhorce valley (Málaga). In: VI Hydrogeology Symposium, Sevilla, 19, pp. 435–447.

Llamas-Dios, M.I., Vadillo-Pérez, I., Candela, L., Jiménez-Gavilán, P., Corada-Fernández, C., Castro-Gámez, A.F., 2020. Screening and distribution of contaminants of emerging concern and regulated organic pollutants in the heavily modified Guadalhorce River basin, southern Spain. Water 12 (11), 3012. https://doi.org/10.3390/w12113012.

Llamas-Dios, M.I., Vadillo-Pérez, I., Jiménez-Gavilán, P., Candela, L., Corada-Fernández, C., 2021. Assessment of a wide array of contaminants of emerging concern in a Mediterranean water basin (Guadalhorce river, Spain): motivations for an improvement of water management and pollutants surveillance. Sci. Total Environ. 788, 147822. https://doi.org/10.1016/j.scitotenv.2021.147822.

Luque Espinar, J.A., Marín Lechado, C., López Geta, J.A., Rubio Campos, J.C., 2003. In: Situación actual de la intrusión en los acuíferos detríticos costeros de Málaga. Tecnología de la Intrusión de agua de mar en acuíferos costeros: países mediterráneos. IGME, Madrid, pp. 713–722 (in Spanish). Ph.D. Thesis.

MAGRAMA, 2012. Characterization of groundwater contamination sources by multi-isotopic techniques. In: Spanish In: Ministry of Environment and Rural and Marine Areas, editor. Internal Report. p. 453.

Martínez, D., Bocanegra, E.M., 2002. Hydrogeochemistry and cation-exchange processes in the coastal aquifer of Mar Del Plata, Argentina. Hydrogeol. J. 10 (3), 393–408. https://doi.org/10.1007/s10040-002-0195-7.

Middelburg, J.J., Van Der Weijden, C.H., Woittiez, J.R.W., 1988. Chemical processes affecting the mobility of major, minor and trace elements during weathering of granitic rocks. Chem. Geol. 68, 253–273. https://doi.org/10.1016/0009-2541(88)90025-3.

Mook, G., 2002. Isótopos ambientales en el ciclo hidrológico. In: Publications of "Instituto Geológico y Minero de España". Guides and Manuals Series, Number 1. IGME, Madrid, Spain, p. 596.

Nadler, A., Margaritz, M., Mazor, E., 1980. Chemical reactions of seawater with rocks and freshwater: experimental and field observations on brackish waters in Israel. Geochim. Cosmochim. Acta 44, 879–886.

Négrel, P., Casanova, J., Aranyossy, J.F., 2001. Strontium isotope systematics used to decipher the origin of groundwaters sampled from granitoids: the Vienne case (France). Chem. Geol. 177 (3–4), 287–308.

Ortí, F., Pérez-López, A., García-veigas, J., Rosell, L., Cendón, D.I., Pérez-Valera, F., 2014. Sulfate isotope compositions (δ34S, δ18O) and strontium isotopic ratios (87Sr/86Sr) of triassic evaporites in the betic cordillera (SE Spain). Rev. Soc. Geol. Esp. 27 (1), 79–90.

Otero, N., Torrentó, C., Soler, A., Menció, A., Mas-Pla, J., 2009. Monitoring groundwater nitrate attenuation in a regional system coupling hydrogeology with multi-isotopic methods: the case of plana de Vic (Osona, Spain). Agric. Ecosyst. Environ. 33, 103–113.

Palmer, M.R., Emond, J.M., 1989. The strotium isotope budget of the modern ocean. Earth Plan. Sci. Lett. 92, 11–26.

Pankina, R.G., 1991. Sulfur isotopic composition of fossil fuels: oil. In: Krouse, H.R., Grinenko, V.A. (Eds.), Stable Isotopes: Natural and Anthropogenic Sulphur in the Environment. Scope. pp. 100–108 (accessed on 10 August 2021).

Parkhurst, D.L., Appelo, C.A., 1999. User's guide to PHREEQC, a computer program for speciation, reaction path, advective–transport, and inverse geochemical calculations. In: Water Resources Investigations Report. US Geological Survey, Reston (VA), pp. 99–4259.

Parkhurst, D.L., Charlton, S.R., 2008. NetpathXL – An Excel Interface to the Program NETPATH. U.S. Geological Survey Techniques and Methods 6-A26, Reston, Virginia.

Petelet-Giraud, E., Negrel, P., Casanova, J., 2003. Variability of 87Sr/86Sr in water draining granite revealed after a double correction for atmospheric and anthropogenic inputs. Hydrol. Sci. J. 48 (5), 729–742.

Plummer, N., Prestemon, E.C., Parkhurst, D.L., 1994. An interactive code (NETPATH) for modeling NET geochemical reactions along a flow PATH, version 2.0. In: U.S. Geological Survey. Water-Resources Investigations Report 94-4169. USGS Earth Science Information Center, Reston – Virginia. https://doi.org/10.3133/wri944169.

Sánchez-García, D., 2010. Water framework directive 2000/60/CE application in the Guadalhorce River Basin (Málaga). In: Initial Characterization. University of Malaga, Malaga, Spain (in Spanish, Ph.D. Thesis, 26th March).

Sánchez-García, D., 2013. In: Aplicación de la Directiva Marco del Agua 2000/60/CE. Caracterización inicial. Public Editorial. p. 656 ISBN 978-3-639-55052-8.

Sánchez-García, D., Vadillo-Pérez, I., Carrasco, F., Mancera, E., 2007. Contamination by agricultural-origin nitrogen compounds within a porous multilayer aquifer in southern Spain. In: Candela, L., Vadillo, I., Aagaard, P., Bedbur, E., Trevisan, M., Vanclooster, M., Viotti, P., López-Geta, J.A. (Eds.), Water Pollution in Natural Porous Media at Different Scales. Assessment of Fate, Impact and Indicators. Instituto Geológico y Minero de España, Madrid, pp. 523–529.

Seal, R.R., 2006. Sulfur isotope geochemistry of sulfide minerals. Rev. Mineral. Geochem. 61 (1), 633–677. https://doi.org/10.2138/rmg.2006.61.12.

Soler, A., Canals, A., Goldstein, S.L., Otero, N., Antich, N., Spangenberg, J., 2002. Sulfur and strontium isotope composition of the Llobregat River (NE Spain): tracers of natural and anthropogenic chemicals in stream waters. Water Air Soil Pollut. 136 (1–4), 207–224.

Spooner, E.T.C., 1976. The strontium isotopic composition of seawater, and seawater-oceanic crust interaction. Earth Planet. Sci. Lett. 31 (1), 167–174. https://doi.org/10.1016/0012-821X(76)90108-4.

Tichomirowa, M., Heidel, C., Junghans, M., Haubrich, F., Matschullat, J., 2010. Sulfate and strontium water source identification by O, S and sr isotopes and their temporal changes (1997–2008) in the region of Freiberg, Central-Eastern Germany. Chem. Geol. 276 (1–2), 104–118.

Urresti-Estala, B., Carrasco-Cantos, F., Vadillo-Pérez, I., Jiménez-Gavilán, P., 2013. Determination of background levels on water quality of groundwater bodies: a methodological proposal applied to a Mediterranean River basin (Guadalhorce River, malaga, southern Spain). J. Environ. Manag. 117, 121–130. https://doi.org/10.1016/j.jenvman.2012.11.042.

Urresti-Estala, B., Vadillo-Pérez, I., Jiménez-Gavilán, P., Soler, A., Sánchez-García, D., Carrasco-Cantos, F., 2015. Application of stable isotopes (δ34S-SO4, δ18O-SO4, δ15N-NO3, δ18O-NO3) to determine natural background and contamination sources in the Guadalhorce River basin (southern Spain). Sci. Total Environ. 506–507, 46–57. https://doi.org/10.1016/j.scitotenv.2014.10.090.

Urresti-Estala, B., Jiménez-Gavilán, P., Vadillo-Pérez, I., Carrasco-Cantos, F., 2016. Assessment of hydrochemical trends in the highly anthropised Guadalhorce River basin (southern Spain) in terms of compliance with the european groundwater directive for 2015. Environ. Sci. Pollut. Res. 23 (16), 15990–16005. https://doi.org/10.1007/s11356-016-6662-9.

Vadillo-Pérez, I., Soler, A., Sánchez-García, D., Carrasco-Cantos, F., 2006. Characterization of sulphate sources by δ34SSO4 and δ18OSO4 for the implementation of European Groundwater Directive in the Guadalhorce river basin (Malaga). In: Hidrogeología y Aguas Subterráneas, 17. Spanish Geological Survey, Madrid, pp. 181–185.

Vadillo-Pérez, I., Jiménez-Gavilán, P., Urresti-Estala, B., Ojeda-Rodríguez, L., Denguir-Bujanow, F., Benavente-Herrera, J., 2019. Application of isotopic techniques for the determination of water sources in the intensive agricultural area of Guadalhorce detrital aquifers (South of Spain). In: International Symposium on Isotope Hydrology Viena (Austria).

Vitòria, L., Otero, N., Soler, A., Canals, A., 2004. Fertilizer characterisation: isotopic data (N, S, O, C and Sr). Environ. Sci. Technol. 38, 3254–3262.

Vitòria, L., Soler, A., Aravena, R., Canals, A., 2005. Multi-isotopic approach (15N, 13C, 34S, 18O and D) for tracing agriculture contamination in groundwater. In: Environmental Chemistry. Springer, Berlin, Heidelberg, pp. 43–56 Chapter 5.

Vitòria, L., Soler, A., Canals, À., et al., 2008. Environmental isotopes (N, S, C, O, D) to determine natural attenuation processes in nitrate contaminated waters: example of osona (NE Spain). Appl. Geochem. 23 (12), 3597–3611.

Vitvar, T., Aggarwal, P.K., McDonnell, J.J., 2005. A review of isotope applications in catchment hydrology. In: Aggarwal (Ed.), Isotopes in the Water Cycle. Editorial Springer, Holanda, pp. 151–169.

Wang, H., Zhang, Q., 2019. Research advances in identifying sulfate contamination sources of water environment by using stable isotopes. Int. J. Environ. Res. Public Health 16 (11), 1914.

Winter, T.C., 1999. Relation of streams, lakes, and wetlands to groundwater flow systems. Hydrogeol. J. 7, 28–45.

Zhang, D., Li, X.D., Zhao, Z.Q., Liu, C.Q., 2015. Using dual isotopic data to track the sources and behaviors of dissolved sulfate in the western North China plain. Appl. Geochem. 52, 43–56.